Research Article | Vol. 8, No. 12 | 1 Dec 2018 | OPTICAL MATERIALS EXPRESS 3635
Optical Materials EXPRESS

Tunable white light emission of a large area film-forming macromolecular complex with a high color rendering index

AIQIN ZHANG,[1,2,5] BIN WANG,[2,3] QIAN YAN,[1,2] YONGCHAO WANG,[1,2] JING JIA,[2,3] HUSHENG JIA,[2,3] BINGSHE XU,[1,2] AND WAI-YEUNG WONG[2,4,6]

[1]*College of Textile Engineering, Taiyuan University of Technology, Taiyuan 030600, China*
[2]*Key Laboratory of Interface Science and Engineering in Advanced Materials, Taiyuan University of Technology, Ministry of Education, Taiyuan 030024, China*
[3]*College of Materials Science and Engineering, Taiyuan University of Technology, Taiyuan 030024, China*
[4]*Department of Applied Biology and Chemical Technology, The Hong Kong Polytechnic University, Hong Kong, China*
[5]*ZAQ6014567@126.com*
[6]*Wai-yeung.wong@polyu.edu.hk*

Abstract: The technological route of pre-polymerization and post-coordination was employed to obtain a rapid film-forming macromolecular complex emitting white light by simultaneously combining poly (styrene-co-glycidyl methacrylate) with three primary color complexes [r(R)/g(G)/b(B)]. The white light emission of the macromolecular complex was realized by tuning the ratios of the trichromatic complexes or altering excitation wavelengths. Upon excitation at 365 nm, macromolecular complex 5 with R:G:B = 1:10:1 exhibits three discrete characteristic peaks at 458 (blue emission), 543 (green emission), and 612 (red emission) nm. The corresponding CIE coordinates of (0.332, 0.337) are in close proximity to pure white light (0.330, 0.330). Macromolecular complex 3 (R:G:B = 1:8:0.5) achieves white emission being excited at the wavelength of 375 nm. Macromolecular complex 5 was melted at 140 °C, dropped on a 365 nm UV chip, and then cooled to room temperature to fabricate an LED device with CIE coordinates of (0.35, 0.34), CCT of 5306 K, and CRI of 95.2. The prepared macromolecular complex film further shows vivid color reproduction for real objects, confirming the high rendering index of the macromolecular complex. In addition, the macromolecular complex remains stable up to 272.6 °C, meeting the requirements of operating temperature for LEDs. This work establishes a rapid film-forming macromolecular complex with potential application in NUV-WLEDs.

1. Introduction

As new solid-state light sources, white light-emitting diodes (WLEDs) have undergone rapid development with extremely promising applications in the field of lighting and display for replacing conventional incandescent and fluorescent lights owing to their superior advantages such as long lifetime, energy saving, high efficiency, light weight, and environmental friendliness [1–3]. WLEDs are easily realized through phosphor converting techniques, in contrast with the high cost and instability of multi-chip technology. Currently, commercially available phosphor-converted white light emitting diodes (pc-WLEDs) are based on a blue chip with yellow emitting phosphor (YAG:Ce^{3+}). However, this approach generates a relatively cool white light with poor color reproduction, which is unsuitable for indoor lighting on account of insufficiency or relatively low intensity of the red component [4]. To circumvent the above drawback, the current focus of fabrication is shifting gradually from blue chip + yellow phosphor to ultraviolet chip + RGB tricolor phosphor by virtue of the invisible emission of the chip and the full gamut of the visible region in the ultraviolet chip +

#340734 https://doi.org/10.1364/OME.8.003635
Journal © 2018 Received 30 Jul 2018; revised 6 Sep 2018; accepted 19 Sep 2018; published 2 Nov 2018

Optical Materials EXPRESS

RGB mode. In recent years, much effort has been devoted to improving the color rendering index (CRI) of phosphor. Unsatisfactorily, significant improvement in this property has not been reached and the CRI is mostly in the range of 80–85 [5–7].

Among the numerous kinds of phosphors, assemblies of lanthanide(III)-containing complexes have attracted considerable attentions for their effective and characteristic luminescence, with generally chosen red (Eu^{3+}, Pr^{3+}, Sm^{3+}), green (Tb^{3+}, Er^{3+}), and blue (Dy^{3+}, Be^{2+}, Ce^{3+}) emissive ions [8–12]. What is worth noting is that most studies have focused on zinc(II) complexes [13] in the research field of blue light emission to replace beryllium(II) complexes, as the latter is too toxic to be applied in practice. Afterwards, small molecular complexes were introduced in the polymer matrix to avoid intrinsic shortcomings such as poor film-forming property in the process of preparation [14]. Wolff et al. [15] solved the film-forming problem for the first time by doping organic rare earth complexes into polymer matrix. Their research results indicated that the polymer matrix had fluorescence enhancement effect on rare earth ions. Since then, several polymers as doped substrates have been investigated [16–18]. However, there are two major drawbacks for doped polymer phosphors. One is the poor compatibility between rare earth complexes and polymers, which gives rise to non-uniform dispersion of complexes in polymer matrix. Another is energy transfer caused by the mutual excitation of rare earth ions. Compared with the doped system, bonding the luminescent ions directly into the polymer chain would overcome the above defects. Hence, many scholars paid their attentions to bonding polymer phosphors. Shunmugam et al. [19] reported a novel white emitting functionalized polymer chelating simultaneously with Eu^{3+}, Tb^{3+}, and Dy^{3+}. Gao et al. [20] bonded naphthoic acid and benzoic acid onto the side chains of polystyrene by polymerization, and coordinated Eu^{3+} or Tb^{3+} ions onto acid-functionalized polystyrenes to prepare binary rare earth macromolecular complexes. However, the most notable problem of technological means—coordinating different rare-earth ions simultaneously with the same functionalized polymer ligand—is a bad match of energy level between one of rare earth ions and molecular ligands. In other words, it is necessary to obtain precursor complexes with better match of energy levels before introduction into polymer matrix. Balamurugan et al. [21] developed a rare earth macromolecular complex emitting white light with CIE coordinates (0.28, 0.34) by coordinating different lanthanide complexes with carboxylic functionalized poly(m-phenylenevinylene). Forster et al. [22] realized the coordination of carbonyl groups present in polycarbonate with rare-earths. Parra et al. [23] reported that Eu^{3+} complex precursor could be immobilized by Eu-O interaction in the polymer matrix diglycidylmetacrylic (DGMA). The mentioned materials realized good matches of energy levels between precursor complexes and matrix, and demonstrated excellent film-forming properties. However, there are few reports about the polymer phosphors of large area film-forming and curing for direct encapsulation.

Herein, we prepared copolymer matrix PS-GMA by the radical polymerization of styrene and glycidyl methacrylate. Subsequently, unsaturated complexes of Eu^{3+}, Tb^{3+}, and Zn^{2+} were coordinated with carbonyl present in the side chain of polymer host to obtain macromolecular complexes. We constructed a series of macromolecular complexes containing Eu^{3+}, Tb^{3+}, and Zn^{2+} displaying a successive change of visible photoluminescence emission color (including white emission) by adjusting the ratio of tricolor monomers. Furthermore, we demonstrated that a UV converted WLED rapidly cured and fabricated with our macromolecular complexes without encapsulating materials, presented CIE chromaticity coordinates (0.33, 0.36), color temperature 5308 K, and color rendering index 95.2. All the results established that the high rendering index macromolecular complex is a material suitable for indoor illumination.

Optical Materials EXPRESS

2. Experimental details

2.1 Materials

$EuCl_3$, $ZnCl_2$, and $TbCl_3$ were purchased from Shanghai Diyang Co. Ltd. 2,2-Azoisobutyronitrile (AIBN), 2-thenoyltrifluoroacetone (TTA), methacrylic acid (MAA), undecylenic acid (UAH), 1,10-phenanthroline (Phen), glycidyl methacrylate (GMA), 4-benzoylbenzoic acid (p-BBA), 2-(2-hydroxyphenyl)benzothiazole (BTZ), and styrene were purchased from Alfa Aesar. All solvents were obtained from Shanghai Chemical Reagent Co. Ltd and used as received without further purification.

2.2 Synthesis of complexes $Eu(TTA)_2(Phen)$, $Tb(p\text{-}BBA)_3$, $Zn(BTZ)$

The complexes were prepared by a method analogous to our earlier work [24]. $Eu(TTA)_2(Phen)$: A solution of 1 mmol $EuCl_3$ in 10 mL ethanol was added dropwise to a solution of 1 mmol Phen in 5 mL ethanol. The pH of the solution was neutralized to 4–5 with 1.0 mol L^{-1} sodium hydroxide ethanol solution. Then, 2 mmol TTA in 5 mL ethanol was added to the mixed solution. The pH of the solution was neutralized to 6–7 by adding 1.0 mol·L^{-1} sodium hydroxide ethanol solution and a large amount of precipitate appeared. The mixed solution was refluxed with stirring at 55 °C for 3 h. The precipitate was collected and repeatedly washed with ethanol. Finally, the product was obtained as solid by drying under vacuum at 80 °C for 24 h. Element analysis (calc.) C 45.11% (45.13%), H 2.86% (2.87%), N 3.33% (3.31%), S 7.54% (7.53%). Yield: 71.95%.

$Tb(p\text{-}BBA)_3$: A solution of 1 mmol $TbCl_3$ in 10 mL ethanol was mixed with a solution of 3 mmol p-BBA in 5 mL ethanol. The mixed solution was heated in a water bath and refluxed with stirring at 55 °C for 3 h. The pH of the solution in the whole process was controlled to 6–7. Finally, the precipitate was collected, repeatedly washed with ethanol, and dried under vacuum at 80 °C for 24 h. Element analysis (calc.) C 59.37% (59.35%), H 5.14% (5.15%). Yield: 62.95%.

Zn(BTZ): A solution of 1 mmol $ZnCl_2$ in 10 mL of ethanol was added dropwise to a solution of 1 mmol BTZ in 5 mL ethanol. The pH of the solution was neutralized to 6–7 with 1.0 mol·L^{-1} sodium hydroxide ethanol solution. The mixed solution was heated in a water bath and refluxed with stirring at 55 °C for 3 h. The precipitate was collected and washed with absolute ethanol. Finally, the product was obtained as solid by drying under vacuum at 80 °C for 24 h. Elemental analysis (calc.) C 61.44% (61.43%), H 7.01% (6.99%), N 2.56% (2.55%), S 6.63% (6.61%). Yield: 72.49%.

The synthesis routes of the complexes are depicted in Fig. 1.

Optical Materials EXPRESS

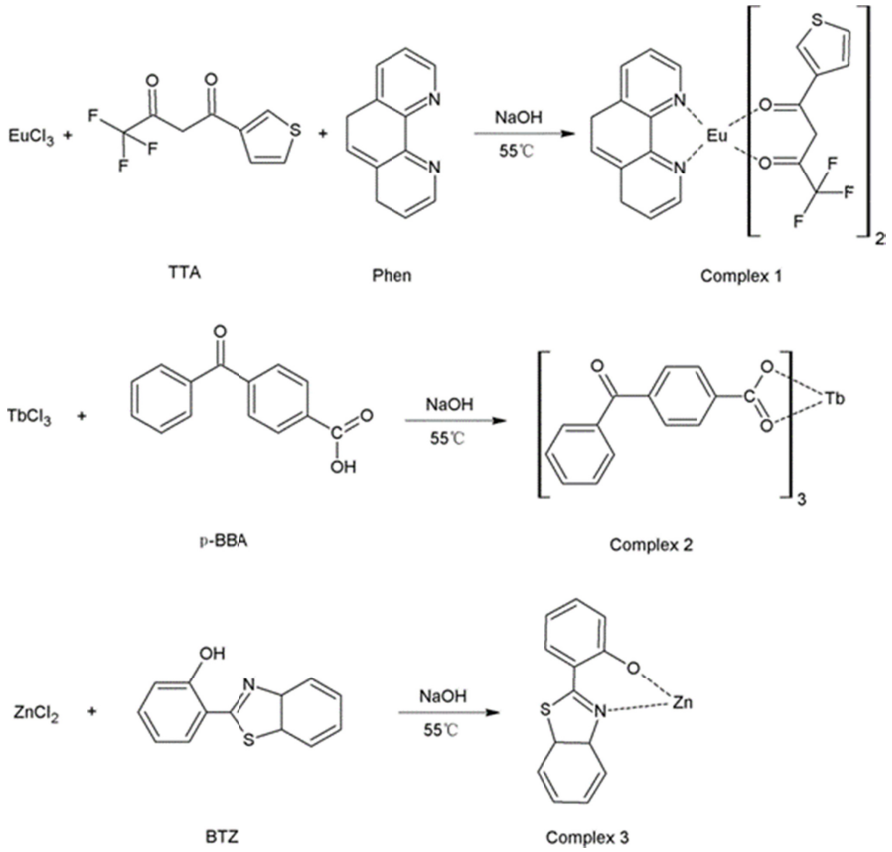

Fig. 1. Synthesis routes of complexes $Eu(TTA)_2(Phen)$, $Tb(p\text{-}BBA)_3$, $Zn(BTZ)$.

2.3 Synthesis of polymer matrix PS-GMA

Tetrahydrofuran solution containing styrene, GMA, and AIBN was transferred to a four-necked flask and mixed with stirring. After dissolution, the solution was bubbled with N_2 for 30 min to remove the O_2 dissolved in the solution. The flask containing the reaction solution was sealed and heated at predetermined temperature for 24 h in a water bath. After polymerization, the resulting solution was precipitated in methanol and filtered off. The crude reaction product was further purified by reprecipitations from acetone to methanol for three times. Finally, the copolymers were dried under vacuum at 50 °C to obtain a white solid powder [25].

The synthesis route of the polymer matrix PS-GMA is depicted in Fig. 2.

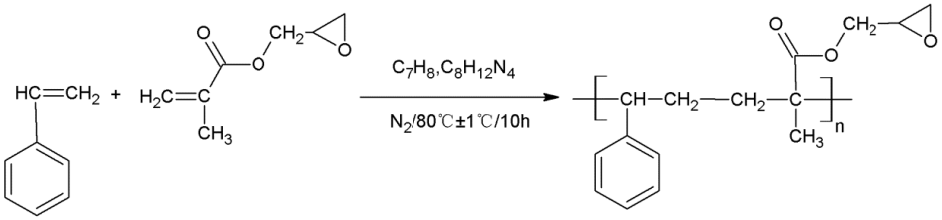

Fig. 2. Synthesis route of polymer matrix PS-GMA.

Optical Materials EXPRESS

2.4 Synthesis of macromolecular complex PS-GMA-Eu-Tb-Zn

A certain mass ratio of PS-GMA, $Eu(TTA)_2(Phen)$, $Tb(p\text{-}BBA)_3$ and Zn(BTZ) was dissolved in 10 mL dimethylsulfoxide solution at 70 °C for 4 h with stirring. The mixture was precipitated out with methanol and further purified by reprecipitations from dimethylsulfoxide to methanol for three times. Finally, the macromolecular complex PS-GMA-$Eu(TTA)_2(Phen)$-$Tb(p\text{-}BBA)_3$-Zn(BTZ)(PS-GMA-Eu-Tb-Zn, for short) was obtained by drying vacuum at 50 °C for 12 h.

The synthesis routes of macromolecular complex PS-GMA-Eu-Tb-Zn are depicted in Fig. 3.

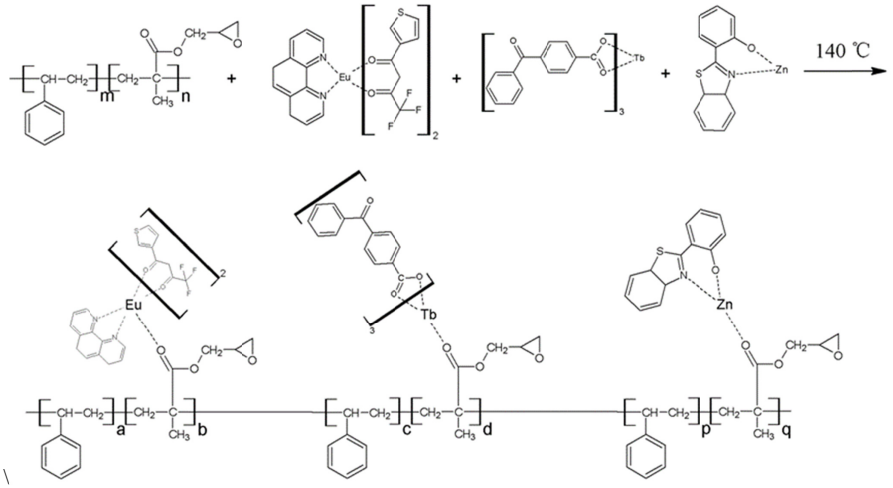

Fig. 3. Synthesis route of macromolecular complex PS-GMA-Eu-Tb-Zn.

2.5 Fabrication of white LEDs

A certain quantity of as-obtained macromolecular complex PS-GMA-Eu-Tb-Zn was added to a crucible and heated at 140 °C on a hot plate stirrer for 10 min until it was completely molten. The molted sample was then softly dripped onto the surface of a UV-chip fixed on a lamp bead, followed by leaving the UV-LED chip coated with macromolecular complex at room temperature for curing. Finally, the polymer optical material was fixed on the surface of a UV-LED chip taking advantage of the epoxy groups to realize the fabrication of WLEDs.

2.6 Preparation of macromolecular complex film

The as-prepared macromolecular complex was ground into fine powder, and filled into a polytetrafluoroethylene (PTFE) mold (80 mm × 80 mm). Subsequently, the PTFE mold filled with phosphor was baked at 140 °C, cured for 30 min at room temperature, and demolded to obtain a polymer film with the size of 80 mm × 80 mm.

2.7 Measurements

Elemental analysis of the complexes was conducted on a Perkin-Elmer Elemental Analyzer. Qualitative analysis of the structures of co-polymer PS-GMA and macromolecular complex PS-GMA-Eu-Tb-Zn was performed using a NICOLET AVATAR 330 Fourier transform infrared (FTIR) spectrometer. UV-vis absorption spectra were measured on a Hitachi-3900 UV-VIS 5 spectrometer. DSC measurement was carried out at a heating rate of 10°C/min under nitrogen on Sapphire Differential Scanning Calorimeter (PerkinElmer). TG analysis was conducted using NETZSCH TG209 F3 with the heating rate of 10°C/min under N_2. Fluorescence spectra and the absolute quantum yield of samples were recorded on an

Optical Materials EXPRESS

Edinburgh LFS-920 spectrometer. Electroluminescence (EL) spectra were obtained on a computer controlled PMS-50 UV-vis-near IR spectrometer with an integrating sphere.

3. Results and discussion

3.1 IR spectra

IR spectra of copolymer PS-GMA and macromolecular complex PS-GMA-Eu-Tb-Zn are given in Fig. 4. The benzene ring vibrations of PS at 1604, 1492, and 1454 cm^{-1} are clearly identified in PS-GMA. The characteristic bands at 908 and 850 cm^{-1} are assigned to the epoxy group [26]. Additionally, the characteristic band at 1726 cm^{-1} is ascribed to the stretching vibration of C = O and the bands at 1182, 1124, and 1074 cm^{-1} are caused by the stretching vibration of C-O-C in the ester group. The above results indicate that copolymer PS-GMA has been synthesized. Furthermore, it is quite clear that the band shape and wavenumber of PS-GMA-Eu-Tb-Zn are basically in accordance with those of PS-GMA, which is due to the low content of complex. Nonetheless, there are some subtle differences between the copolymer PS-GMA and macromolecular complex PS-GMA-Eu-Tb-Zn. The characteristic bands in PS-GMA-Eu-Tb-Zn at 445 and 418 cm^{-1} are attributed to the stretching vibration of Eu-O in the complex $Eu(TTA)_2(Phen)$ and Tb-O in the complex $Tb(p\text{-}BBA)_3$, respectively. Besides, the weak band at 472 cm^{-1} is caused by the interaction between metallic Zn^{2+} and carbonyl group in the side chain of GMA chain segment [27]. All of these results imply that the three primary complexes have coordinated with the carbonyl group from the GMA chain segment in the polymer PS-GMA.

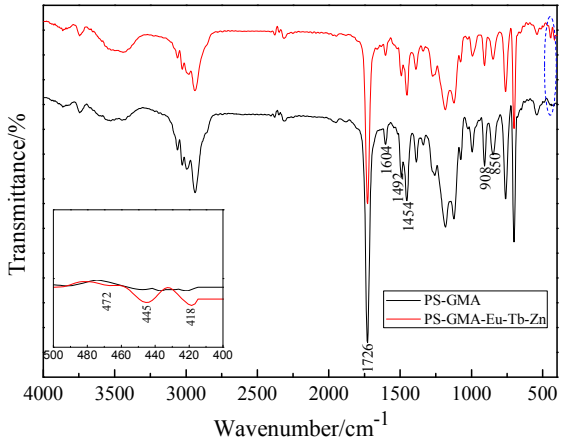

Fig. 4. IR spectra of copolymer PS-GMA and macromolecular complex PS-GMA-Eu-Tb-Zn.

3.2 UV-vis absorption spectra

UV-vis absorption spectra of polymer PS-GMA and polymer PS-GMA-Eu-Tb-Zn in DMF are shown in Fig. 5(a). In comparison, UV-vis absorption spectra of complex $Eu(TTA)_2(Phen)$, $Tb(p\text{-}BBA)_3$, and Zn(BTZ) are presented in Fig. 5(b). In polymer PS-GMA, the strong absorption peak centered at 271 nm originates from the K absorption band of the benzene ring in the PS segment. In polymer PS-GMA-Eu-Tb-Zn, the K absorption band of the benzene ring becomes stronger than that in PS-GMA, and this is due to enhancement of the n-π* absorption (270 nm) of C = N in the BTZ of complex Zn(BTZ) [28]. Moreover, two broad absorption peaks at 279 and 334 nm are observed in PS-GMA-Eu-Tb-Zn. The former mainly comes from the π-π* transition of the conjugate structure between the benzene ring and the carboxyl or carbonyl group in complex $Tb(p\text{-}BBA)_3$ [29]. The latter was ascribed to the joint effect of the absorption of the ketonic form of TTA in complex $Eu(TTA)_2(Phen)$ and intramolecular charge transition from the phenol ring to the benzothiazole unit in complex

Optical Materials EXPRESS

Zn(BTZ) [30]. The above analysis reveals that the complexes are effectively coordinated with the copolymer PS-GMA.

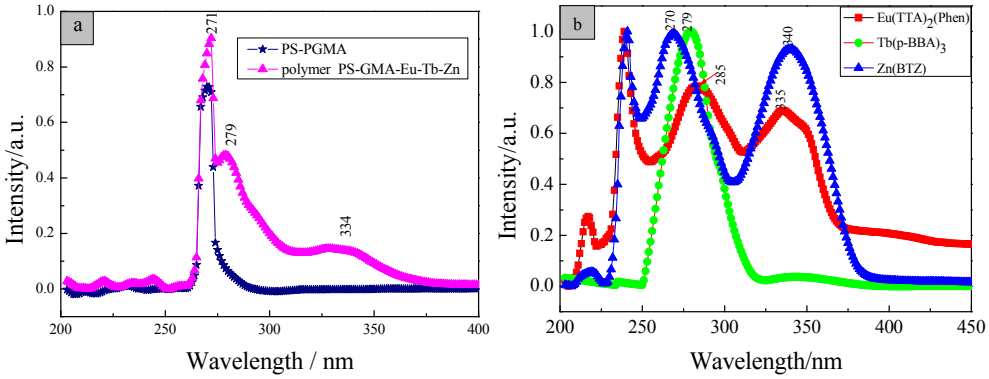

Fig. 5. UV-vis absorption spectra of complexes $Eu(TTA)_2(Phen)$, $Tb(p\text{-}BBA)_3$, and Zn(BTZ), polymer PS-GMA, and polymer PS-GMA-Eu-Tb-Zn.

3.3 Thermal properties

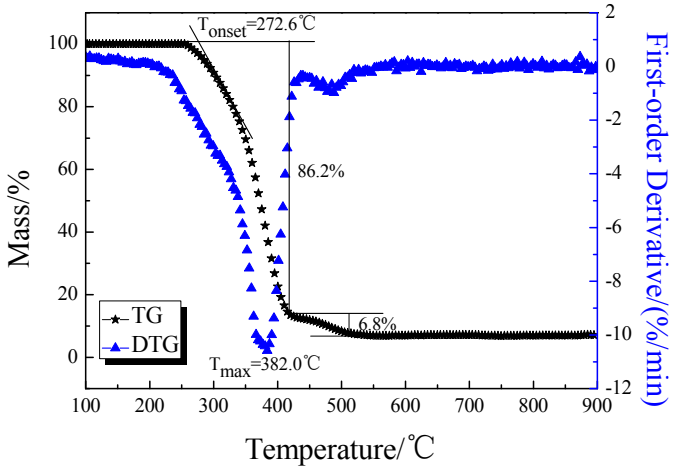

Fig. 6. TG-DTG curves of polymer PS-GMA-Eu-Tb-Zn.

Thermogravimetric (TG) analysis of polymer PS-PGMA-Eu-Tb-Zn in the temperature range of 100 °C to 900 °C was conducted at heating rate 10 °C/min under nitrogen. A first-order derivative curve (DTG) was fitted with the Origin 8.0 software package. The results are illustrated in Fig. 6. Apparently, the thermal decomposition process is divided into two stages. The first weight loss occurs at 272.6–413.0 °C with weight loss 86.2% and the weight loss rate reaches the maximum at 382.0 °C, occurring at this decomposition stage. In this stage, the decomposition changes gently probably owing to the decomposition of copolymers with low molecular weight and the partial removal of small molecule ligands and decomposition of the polymer skeleton chain. The second weight loss occurs at 418.6–545.2°C with a tiny weight loss of 6.8% attributed to complete decomposition of complexes, which further confirms the coordination between metal ions and ligands. The results suggest that the polymer keeps stable up to 272.6 °C. In view of operating temperatures of LEDs below 150 °C [31], the macromolecular complex is thermally stable for the requirement of LEDs.

Optical Materials EXPRESS

3.4 Photoluminescence properties

The excitation and emission spectra of complexes $Eu(TTA)_2(Phen)$, $Tb(p\text{-}BBA)_3$, and Zn(BTZ) in the solid state recorded at room temperature with slit width 1 nm are presented in Fig. 7. The excitation spectrum of $Eu(TTA)_3$ (see Fig. 7(a)) obtained by monitoring the emission of Eu(III) ion at 612 nm shows a broad absorption peak from 240 nm to 500 nm with a maximum at 325 nm, which is caused by π-π* transition of the TTA ligand [32]. Upon excitation at a wavelength of 365 nm, the emission spectrum of the complex exhibits characteristic emissions at 579, 590, 612, and 649 nm attributed to the $^5D_0$-$^7F_0$, $^5D_0$-$^7F_1$, $^5D_0$-$^7F_2$, and $^5D_0$-$^7F_3$ transitions, respectively. Among them, the dominant peak at 612 nm results in pure red emission. In Fig. 7(b), the excitation spectrum of $Tb(p\text{-}BBA)_3$ monitored at 543 nm similarly shows a broad band from 240 nm to 400 nm centered at 362 nm due to intramolecular charge transfer in the p-BBA ligand [33]. Being excited at 365 nm, the complex $Tb(p\text{-}BBA)_3$ presents four characteristic emissions at 488, 542, 582, and 619 nm, ascribed to $^5D_4$-$^7F_6$, $^5D_4$-$^7F_5$, $^5D_4$-$^7F_4$, and $^5D_4$-$^7F_3$ transitions of Tb^{3+}, respectively. Obviously, pure green emission is the result of the dominant peak at 542 nm. The complex Zn(BTZ) shows a typical blue emission peak centered at 472 nm when excited at 365 nm (Fig. 7(c)). The excitation spectrum displays a broad band with maximum at 367 nm when monitored at 450 nm. The above results suggest that the complexes $Eu(TTA)_2(Phen)$, $Tb(p\text{-}BBA)_3$, and Zn(BTZ) can be qualified as three primary colors to be mixed in proper proportion for white light emission upon excitation at 365 nm.

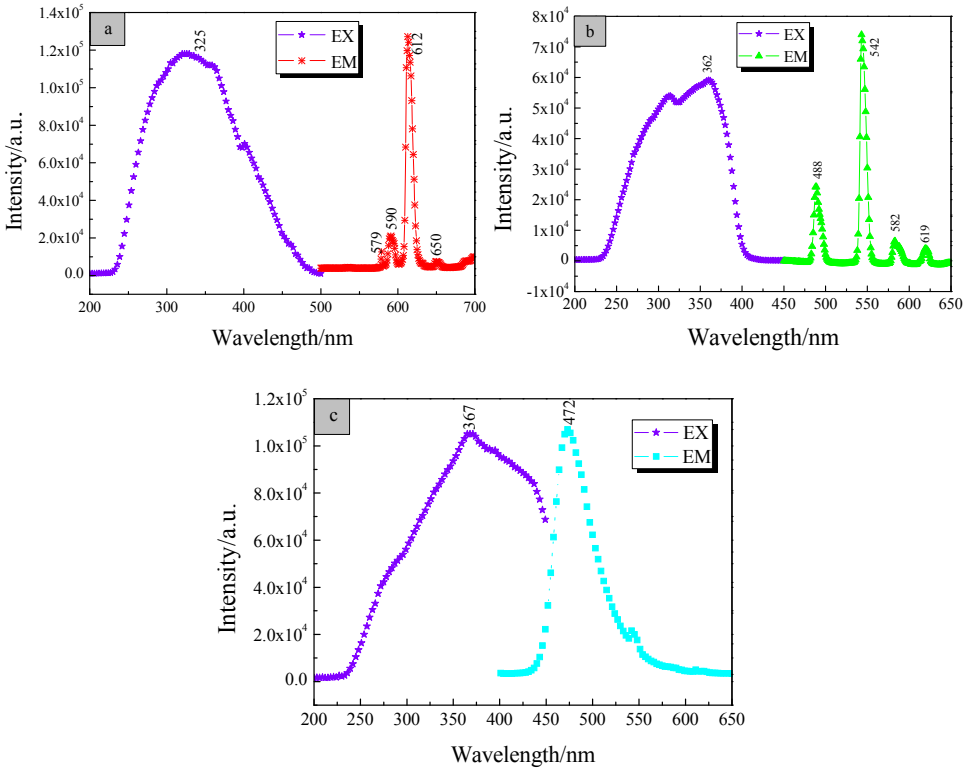

Fig. 7. Fluorescence spectra of complex $Eu(TTA)_2(Phen)$ (a), Tb $(p\text{-}BBA)_3$ (b), and Zn(BTZ) (c).

Optical Materials EXPRESS

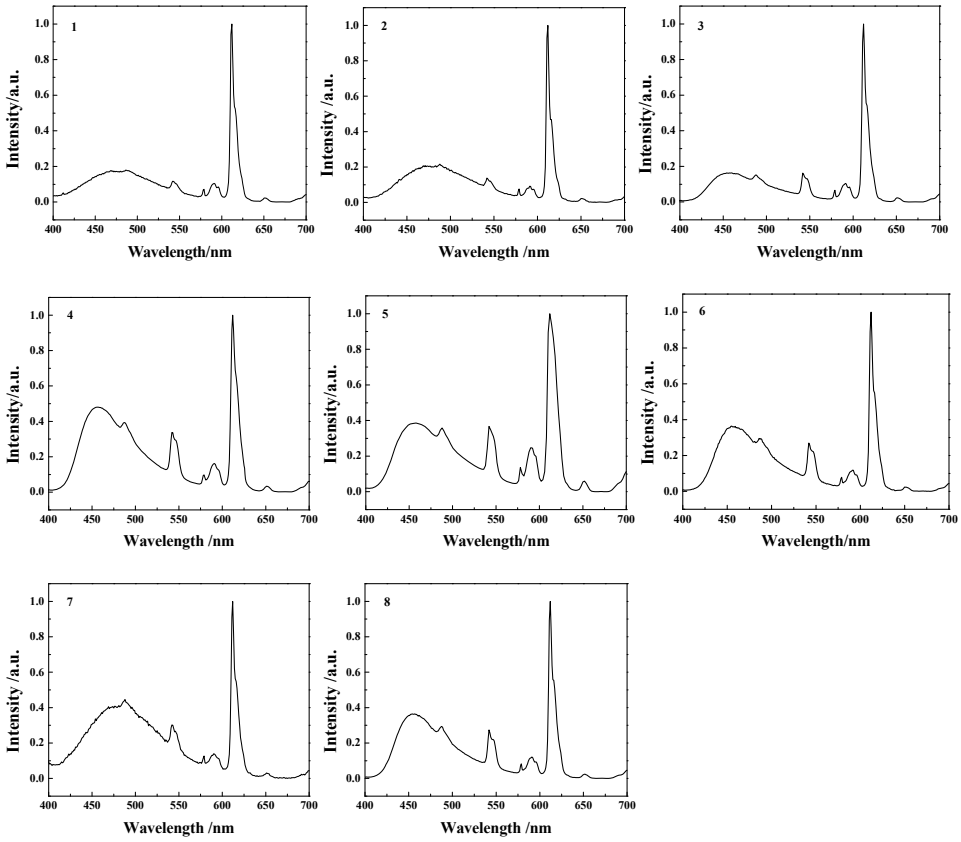

Fig. 8. Emission spectra of polymer PS-GMA-Eu-Tb-Zn (the RGB ratios:(1) 1:2:0.5; (2) 1:4:0.5; (3) 1:8:0.5; (4) 1:9:1; (5) 1:10:1; (6) 1:15:1; (7) 1:20:2; (8) 1:25:2) excited at 365 nm.

The emission spectra of polymers PS-GMA-Eu-Tb-Zn 1-8 with different molar ratios upon excitation wavelength at 365 nm are illustrated in Fig. 8. The corresponding CIE chromaticity coordinates are calculated from the emission spectra and marked in Fig. 9. All the polymers display blue, green, and red characteristic emissions attributed to the complexes Zn(BTZ),Tb(p-BBA)$_3$, Eu(TTA)$_2$(Phen). It is observed that the coordinates travel through the light pink area while shifting from pink to the white light zone. It's gratifying to see that the CIE chromaticity coordinates of samples 4, 5, 6, and 7 distribute in the white light zone, which are realized by changing the contents of the green and blue complexes. Among the coordinates of the white light region, (0.332, 0.337) of sample 5 is optimal under excitation at 365 nm, which is very close to pure white light at (0.330, 0.330), according to the 1931 CIE coordinate diagram.

Optical Materials EXPRESS

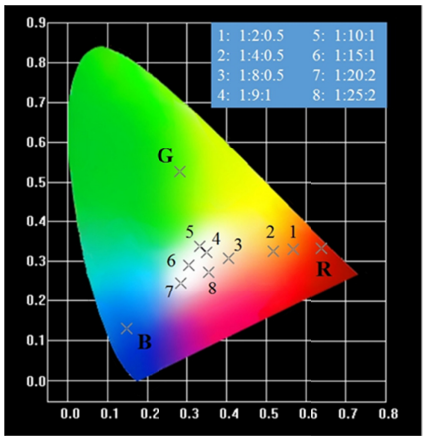

Fig. 9. CIE chromaticity coordinates for the three primary colors complexes and polymer PS-GMA-Eu-Tb-Zn excited at 365 nm [R: (0.641,0.332), G: (0.283,0.524), B: (0.147,0.130)].

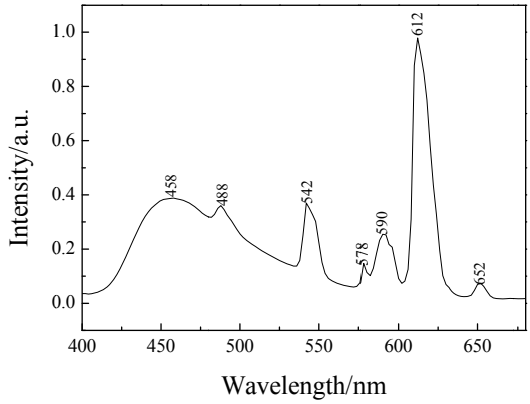

Fig. 10. Emission spectrum of polymer PS-GMA-Eu-Tb-Zn with RGB ratio 1:10:1 excited at 365 nm.

Figure 10 presents the fluorescence emission spectrum of polymer PS-GMA-Eu-Tb-Zn with RGB ratio 1:10:1 at excitation wavelength of 365 nm. It is noted that the polymer exhibits not only typical peaks at 578, 590, 612, and 652 nm corresponding to $^5D_0$-$^7F_0$, $^5D_0$-$^7F_1$, $^5D_0$-$^7F_2$, and $^5D_0$-$^7F_3$ transitions of Eu^{3+} in complex $Eu(TTA)_2(Phen)$, respectively, but also characteristic peaks at 488 and 542 nm ascribed to $^5D_4$-$^7F_6$ and $^5D_4$-$^7F_5$ transitions of Tb^{3+} in complex $Tb(p\text{-}BBA)_3$, respectively. Nonetheless, the characteristic emission spectra of the polymer show broadened peaks of Eu^{3+} and Tb^{3+} in contrast with those of the complex $Eu(TTA)_2(Phen)$ and complex $Tb(p\text{-}BBA)_3$, indicating the coordination between Eu^{3+}, Tb^{3+}, and PS-GMA polymer matrix [22]. Besides, the broadband emission in the range of 400–480 nm centered at 458 nm has a blue shift of about 14 nm relative to the emission spectrum of the complex Zn(BTZ). This may be caused by the decreased cloud expansion effect surrounding the complex after coordination between Zn^{2+} and the carbonyl group in the polymer matrix [34].

To intuitively and vividly show the gradual change in color regulation, macromolecular complex in the shape of a wafer was prepared; Luminescent photograph of macromolecular complex 1-8 excited at 365 nm are shown in Fig. 11. It is distinct that their emissions gradually changes from pink to tin white, which is in accordance with their CIE chromaticity coordinates.

Optical Materials EXPRESS

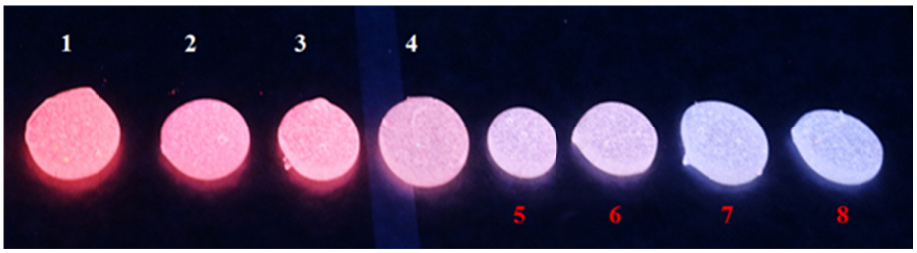

Fig. 11. Luminescent photograph of macromolecular complex 1-8 excited at 365 nm.

Apart from the polymer with RGB ratio 1:10:1, other serial macromolecular complexes can be also obtained white light emission by altering excitation wavelength. For example, the emission spectrum of macromolecular complex with RGB ratio 1:8:0.5 monitored at 355–385 nm is depicted in Fig. 12. As the excitation wavelength varies from 355 to 385 nm, there are always six emission peaks at around 458, 488, 542, 578, 590, and 612 nm. The shift in the emission peak is barely noticeable, that is to say, the peak position is not affected by the change in excitation wavelength, which is consistent with previous work [35,36]. Despite this, the peak intensities depend mainly on excitation wavelength. In particular, the blue emission increases monotonically with increasing excitation wavelength. However, the green emission (542 nm) first increases and then decreases. This is due to the fact that the maximum excitation wavelength centers at 362 nm in the complex $Tb(p\text{-}BBA)_3$ and the excitation intensity declines sharply from 362 nm to 385 nm, which results in the initial increases and later decreases with increasing excitation wavelength from 355 nm to 385 nm. In the case of complex $Eu(TTA)_2(Phen)$, the excitation broadband is located in the range 230–500 nm (centered at 325 nm) and the excitation intensity vary slightly from 355 to 385 nm. Therefore, the Eu^{3+} ion has the increased emission from 355 to 380 nm and a drop at 385 nm. It is noted that the emission intensity doesn't strictly conform to the excitation intensity of the corresponding complex. It can be derived that energy transfer occurs from the Tb^{3+} ion to the Eu^{3+} ion.

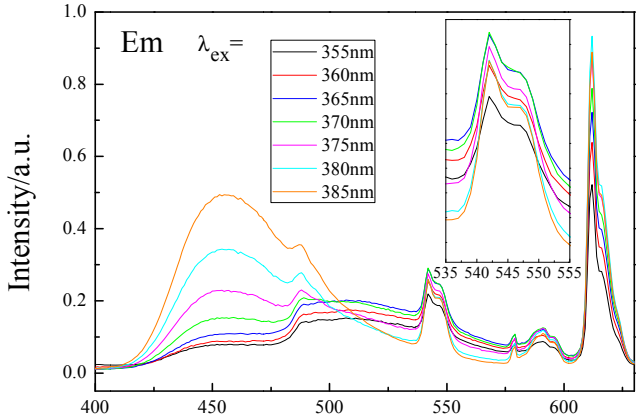

Fig. 12. Emission spectra of polymer with RGB ratio 1:8:0.5 monitored at excitation wavelengths 355–385 nm.

It is feasible to tune the chromaticity of the emission color of the samples to realize white light emission by selecting a proper excitation wavelength. The corresponding CIE chromaticity coordinates in Fig. 13 based on the PL results vividly reflect color regulation by altering the excitation wavelength from 355 nm to 385 nm. The x value of the CIE chromaticity coordinates of the polymer gradually decreases with the increase of the excitation wavelength, and the corresponding coordinates vary gradually from yellowish pink

Optical Materials EXPRESS

(0.473, 0.314) to greenish blue (0.208, 0.271) from 355 nm to 385 nm. The optimal CIE coordinates (0.336, 0.301) of the polymer excited at 375 nm is located in the white light area.

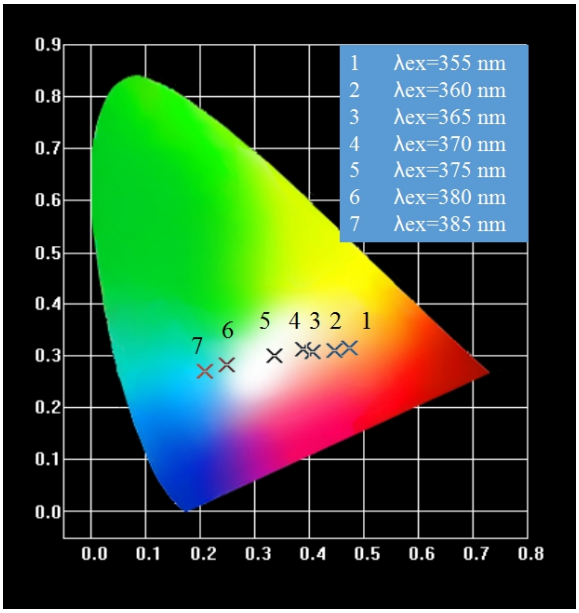

Fig. 13. CIE chromaticity coordinates for polymer with RGB ratio 1:8:0.5 at excitation wavelengths of 355–385 nm [1: (0.473, 0.314), 2: (0.446, 0.311), 3: (0.405, 0.307), 4: (0.387, 0.313), 5: (0.336, 0.301), 6: (0.248, 0.282), 7: (0.208, 0.271)].

3.5 Quantum yield and fluorescence lifetime

The quantum yield (η_s) of the polymer with RGB ratio 1:10:1 at room temperature was also measured in 10^{-3} mol·L^{-1} DMF solution and calculated according to Eq. (1) using $Eu(TTA)_3(phen)$ as reference.

$$\eta_s = \eta_R \frac{A_R I_s N_s^2}{A_s I_R N_R^2} \tag{1}$$

where $\eta_R = 0.365$ is the quantum yield of $Eu(TTA)_3phen$ in 10^{-3} mol·L^{-1} DMF [37]. A, I and N denote the area of the emission spectrum, the absorbance intensity at the excitation wavelength, and the refractive index of the solvent, respectively. The refractive index N_S is equal to N_R under the condition of the same DMF solution used for measurement. The quantum yield (η_s) of the macromolecular complex is calculated as 0.112.

As one of the significant indicators of luminescent performance, fluorescence lifetime was measured in the solid state at room temperature obtained by fitting luminescence decay data to the double exponential Eq. (2).

$$I(t) = A + B_1 \exp(-t/\tau_1) + B_2 \exp(-t/\tau_2) \tag{2}$$

where τ_1 and τ_2 are the shorter and longer lifetime components, respectively. B_1 and B_2 are fitting constants. The average lifetime $\langle\tau\rangle$ is given by Eq. (3).

$$\langle\tau\rangle = \frac{B_1\tau_1^2 + B_2\tau_2^2}{B_1\tau_1 + B_2\tau_2} \tag{3}$$

Optical Materials EXPRESS

Figure 14 presents the fluorescence decay curve and its fitted curve of $^5D_0$-$^7F_2$ transition of Eu^{3+} ion recorded at the excitation wavelength of 612 nm. For $^5D_0$-$^7F_2$ transition of Eu^{3+} ion, the parameters in Eq. (3) are as follows, A = 0.605, B_1 = 296.92, B_2 = 133.70, τ_1 = 11.87 us, τ_2 = 629.78 us, and the average lifetime $\langle\tau\rangle$ is calculated on the basis of Eq. (3) as 0.732 ms.

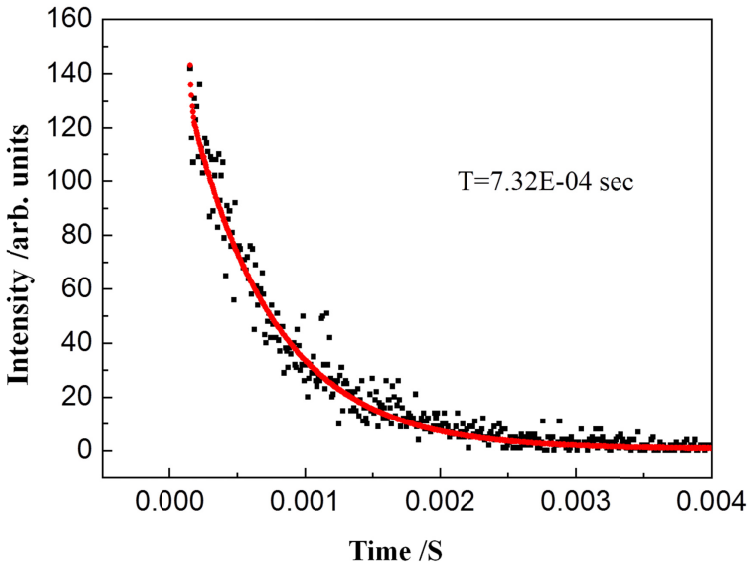

Fig. 14. Fluorescence lifetime decay curve of the polymer with RGB ratio 1:10:1 monitored at the $^5D_0$-$^7F_2$ transition (black dots) and fitted curve (red line).

3.6 WLED fabricated with polymer PS-GMA-Eu-Tb-Zn with RGB ratio 1:10:1

In order to further demonstrate its potential use in WLED devices, the macromolecular complex was encapsulated in 1 W lamp beads with a 365 nm UV-chip. The EL spectrum of the fabricated WLED device driven at 350 mA is given in Fig. 15. The corresponding CIE chromaticity coordinates are marked in Fig. 16 and the inset is the practical emission profile of the fabricated WLED. The EL spectrum of the WLED lamp at 350 mA displays characteristic peaks at 470, 545, and 615 nm, attributed to blue, green, and red emission from complex Zn(BTZ), complex Tb(p-BBA)$_3$, and complex Eu(TTA)$_2$(Phen), respectively. The CIE chromaticity coordinates originating from the EL spectrum are (0.35, 0.34), which is roughly consistent with (0.332, 0.337) from the PL spectrum. Compared with the PL spectrum, the EL spectrum has minor deviation of chromaticity coordinates, suggesting the luminescent stability of phosphor when fabricated into white LEDs.

Optical Materials EXPRESS

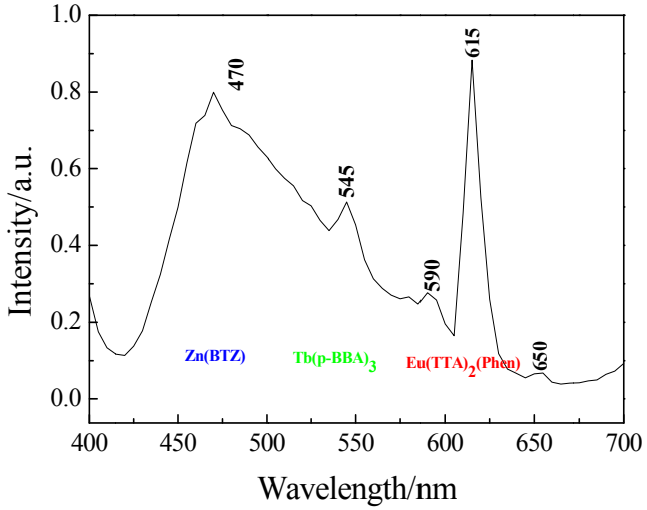

Fig. 15. EL spectrum of the WLED fabricated with macromolecular complex driven at 350 mA.

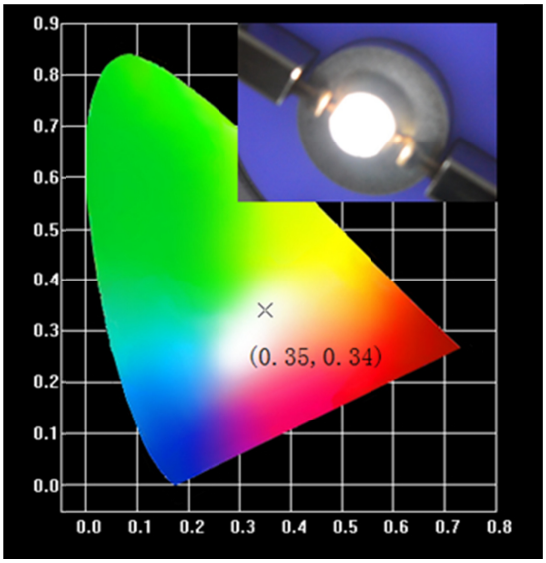

Fig. 16. CIE chromaticity coordinates of the WLED calculated from EL spectrum; inset is the profile of the WLED driven by 350 mA.

The fabricated WLED has a low CCT of 5306 K and high CRI of 95.2 compared with WLEDs based on the reported polymer phosphors (CRI = 83.5, CCT = 5600 K) [27] or WLED combining blue InGaN chip and YAG:Ce^{3+} phosphor (CRI = 75, CCT = 7756 K) [38] or pc-WLEDs combining three color phosphors (blue, green, and red) with near-ultraviolet LED chips(CRI = 93.8, CCT = 4606 K) [39]. The luminous efficiency is 103 lm/W. This is because the additional introduction of the red component on the basis of generating white light through the complement of two primary colors contributed to the full gamut of the visible region. A high RGB spectral proportion is contributed to a promoting the efficiency of converting UV light to white light, which favors a high CRI value in white LEDs [40]. Furthermore, besides these strongest characteristic peaks, other peaks also have certain intensities, which are also beneficial to the improvement of the color rendering index. Thus,

Optical Materials EXPRESS

the feature of high RGB proportion would make the as-prepared macromolecular complex suitable for phosphor application in white LEDs.

Since the limited light emitting area of as-fabricated WLEDs is incapable of intuitively showing vivid color reduction for the illuminated object, we prepared a flat luminescent panel with macromolecular complex 5 via melting solidification. Figure 17(a) is a digital photograph of the practical emission of the macromolecular complex film cured in PTFE mold (80 mm × 80 mm) excited at 365 nm. This suggests that this kind of macromolecular complex is adequate to directly formation of a film for a large area fluorescent screen. Figure 17(b) shows a photo of seven-color candies irradiated at UV light of 365 nm. Figure 17(c) shows a photo of seven-color candies under the radiation from a large size (80 mm × 80 mm) photo of a macromolecular complex film excited at 365 nm, in which excellent color rendering capability is demonstrated by vivid color reproduction of the seven-color candies.

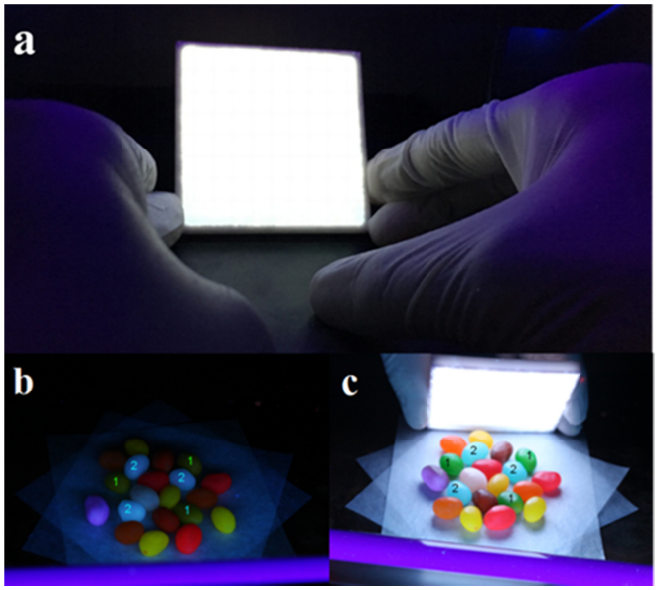

Fig. 17. Photo of a large area (80 mm × 80 mm) polymer white emitting film excited at 365 nm (a). Photo of seven-color candies irradiated at UV light of 365 nm (b). Photo of seven-color candies under the radiation from a large area (80 mm × 80 mm) polymer film excited at 365 nm (c).

Comparison of Fig. 17(b) with Fig. 17(c) shows that the same candies turn out to be of distinctively different colors with and without the polymer white light film, especially candies numbered 1 and 2. In Fig. 17(b), candy 1 with a green color and candy 2 with a blue color show yellowish-brown and silvery white under the irradiation of 365 nm UV lamps. To our great satisfaction, in Fig. 17(c), candy 1 and 2 show their really colors under the radiation of the polymer white light film. Besides, candies with other colors like yellow, orange, and red all appear in their actual colors.

Obviously, these kinds of macromolecular complexes satisfy the illumination requirements and are promising optical materials for applications in indoor lighting. Meanwhile, the macromolecular complex in molten state has the property of rapid self-curing at room temperature, which can be applied in the fabrication of WLED directly from this kind of macromolecular complex instead of the complicated process of mixing with packaging adhesive and long cure times currently required for conventional LED encapsulation.

Optical Materials EXPRESS

4. Conclusions

In this work, a rapidly curing macromolecular complex has been developed using the technical route of pre-polymerization and post-coordination. White light emission was realized through two kinds of technical schemes (adjusting the ratio of R/G/B complexes or altering the excitation wavelength). Macromolecular complex 3 achieves white emission being excited at 375 nm. The macromolecular complex with the ratio of R:G:B = 1:10:1 exhibits three discrete characteristic peaks at 458 (blue emission), 543 (green emission), and 612 (red emission) nm, respectively. The corresponding CIE coordinates of (0.332, 0.337) are in close proximity to pure white light (0.330, 0.330). WLED fabricated with macromolecular complex 5 shows applicable CCT of 5306 K, excellent CRI of 95.2, and luminous efficiency of 103 lm/W being driven at 350 mA. The CIE coordinates from the EL spectrum are (0.35, 0.34), similar to the PL spectrum, maintaining the original luminous performance. The prepared macromolecular complex film further shows the vivid color reproduction of real objects, confirming the high rendering index of the macromolecular complex. The results suggest that the macromolecular complex saves the trouble of mixing with packaging adhesive and curing for long times in conventional LED encapsulation. In addition, the macromolecular complexes keep stable until 272.6 °C, meeting the requirements for the operating temperature (180 °C) of LEDs. Our findings demonstrate that the macromolecular complexes have potential applications in NUV-WLEDs.

Funding

National Natural Science Foundation of China (NSFC) (21471111); Shanxi Natural Science Foundation of China (SNSFC) (201601D102020); Shanxi Key Research and Development Program of China (SKRDPC) (201603D121017); Hong Kong Polytechnic University (AGHKPU) (1-ZE1C) (AOEC Grant).

References

1. S. Huang, Y. Chen, X. Wei, and M. Yin, "Synthesis and luminescence properties of $NaSrPO_4:Eu^{2+}$, Tb^{3+}, Mn^{2+} for WLED," J. Nanosci. Nanotechnol. **14**(6), 4574–4578 (2014).
2. H. S. Jang and D. Y. Jeon, "White light emission from blue and near ultraviolet light-emitting diodes precoated with a $Sr_3SiO_5:Ce^{3+}$,Li+ phosphor," Opt. Lett. **32**(23), 3444–3446 (2007).
3. G. B. Nair and S. J. Dhoble, "White Light Emitting $MZr_4(PO_4)_6:Dy^{3+}$ (M = Ca, Sr, Ba) Phosphors for WLEDs," J. Fluoresc. **27**(2), 575–585 (2017).
4. X. Jiang, Z. Chen, S. Huang, J. Wang, and Y. Pan, "A red phosphor $BaTiF_{(6)}:Mn^{(4+)}$: reaction mechanism, microstructures, optical properties, and applications for white LEDs," Dalton Trans. **43**(25), 9414–9418 (2014).
5. M. Shang, C. Li, and J. Lin, "How to produce white light in a single-phase host?" Chem. Soc. Rev. **43**(5), 1372–1386 (2014).
6. Y. Jin, M. H. Fang, M. Grinberg, S. Mahlik, T. Lesniewski, M. G. Brik, G. Y. Luo, J. G. Lin, and R. S. Liu, "Narrow Red Emission Band Fluoride Phosphor $KNaSiF_6:Mn^{4+}$ for Warm White Light-Emitting Diodes," ACS Appl. Mater. Interfaces **8**(18), 11194–11203 (2016).
7. D. Zhou, M. Liu, M. Lin, X. Bu, X. Luo, H. Zhang, and B. Yang, "Hydrazine-mediated construction of nanocrystal self-assembly materials," ACS Nano **8**(10), 10569–10581 (2014).
8. H. Y. Lin, Y. C. Fang, and S. Y. Chu, "Energy Transfer $Sm^{3+}\rightarrow Eu^{3+}$ in Potential Red Phosphor $(Ca, Ba)_3(VO_4)_2:Sm^{3+}$, Eu^{3+} for Use in Organic Solar Cells and White Light-Emitting Diodes," J. Am. Ceram. Soc. **93**(11), 3850–3856 (2010).
9. Y. H. Won, H. S. Jang, W. Bin Im, and D. Y. Jeon, "Red-emitting $LiLa_2O_2BO_3$: Sm^{3+}, Eu^{3+} phosphor for near-ultraviolet light-emitting diodes-based solid-state lighting," J. Electrochem. Soc. **155**(9), J226–J229 (2008).
10. Z. H. Zhang, Y. H. Wang, and X. X. Li, "Synthesis and Photoluminescence of Green-Emitting X_2-$(Y,Gd)_2Sio_5:Tb^{3+}$ Phosphor under Vuv Excitation," Biolum. Chemilum. **13**, 329–332 (2009).
11. O. Toma, E. Osiac, and S. Georgescu, "Pump wavelengths for an Er: $YLiF_4$ green-emitting laser," Opt. Mater. **30**(1), 181–183 (2007).
12. A. B. Canaj, D. I. Tzimopoulos, A. Philippidis, G. E. Kostakis, and C. J. Milios, "A Strongly Blue-Emitting Heptametallic $[Dy^{III}_7]$ Centered-Octahedral Single-Molecule Magnet," Inorg. Chem. **51**(14), 7451–7453 (2012).
13. C. Zitzer, T. W. T. Muesmann, J. Christoffers, and M. S. Wickleder, "Crystal Engineering with the New Linker Tolanedisulfonic Acid (H_2 TDS): Helical Chains in $Zn(TDS)(DMA)_3$, Linear Chains in $Zn(TDS)(NMP)_3$, and Complex Anions in $[HDMA]_2$ $[Zn(TDS)_2$ $(DMA)_3$ $](DMA)_2$," Chem. Asian J. **10**(6), 1354–1362 (2015).
14. A. Q. Zhang, X. D. Hao, J. L. Zhang, H. S. Jia, X. G. Liu, and B. S. Xu, "Tuning of the emission chromaticity of Eu, Gd, Be-containing copolymers," Opt. Mater. **37**, 5–10 (2014).

Optical Materials EXPRESS

15. N. E. Wolff and R. J. Pressley, "Optical master action in Eu^{3+} containing organic matrix," Appl. Phys. Lett. **2**(8), 152–154 (1963).
16. J. Kai, D. F. Parra, and H. F. Brito, "Polymer matrix sensitizing effect on photoluminescence properties of Eu^{3+}-beta-diketonate complex doped into poly-beta-hydroxybutyrate (PHB) in film form," J. Mater. Chem. **18**(38), 4549–4554 (2008).
17. D. B. A. Raj, B. Francis, M. L. P. Reddy, R. R. Butorac, V. M. Lynch, and A. H. Cowley, "Highly Luminescent Poly(Methyl Methacrylate)-Incorporated Europium Complex Supported by a Carbazole-Based Fluorinated β-Diketonate Ligand and a 4,5-Bis(diphenylphosphino)-9,9-dimethylxanthene Oxide Co-Ligand," Inorg. Chem. **49**(19), 9055–9063 (2010).
18. L. Zhang, J. Zhang, G. H. Pan, X. Zhang, Z. Hao, Y. Luo, and H. Wu, "Low-Concentration Eu^{2+}-Doped $SrAlSi_4N_7$: Ce^{3+} Yellow Phosphor for wLEDs with Improved Color-Rendering Index," Inorg. Chem. **55**(19), 9736–9741 (2016).
19. R. Shunmugam and G. N. Tew, "Dialing in color with rare earth metals: facile photoluminescent production of true white light," Polym. Adv. Technol. **18**(11), 940–945 (2007).
20. B. Gao, N. Shi, and Z. Qiao, "Structure and luminescent property of complexes of aryl carboxylic acid-functionalized polystyrene with Eu(III) and Tb(III) ions," Spectrochim. Acta A Mol. Biomol. Spectrosc. **150**, 565–574 (2015).
21. A. Balamurugan, M. L. P. Reddy, and M. Jayakannan, "Single Polymer Photosensitizer for Tb^{3+} and Eu^{3+} Ions: An Approach for White Light Emission Based on Carboxylic-Functionalized Poly(m-phenylenevinylene)s," J. Phys. Chem. B **113**(43), 14128–14138 (2009).
22. P. L. Forster, D. F. Parra, J. Kai, D. M. Fermino, H. F. Brito, and A. B. Lugao, "Effects of gamma radiation on the photoluminescence properties of polycarbonate matrices doped with terbium complex," Radiat. Phys. Chem. **79**(3), 347–349 (2010).
23. D. F. Parra, H. F. Brito, and A. B. Lugao, "Influence of the gamma irradiation on photoluminescence properties of DGMA doped with Eu3+-beta-diketonate complex," Nucl. Instrum. Meth. B **236**(1–4), 235–240 (2005).
24. A. Q. Zhang, J. L. Zhang, Q. L. Pan, S. H. Wang, H. S. Jia, and B. S. Xu, "Synthesis, photoluminescence and intramolecular energy transfer model of a dysprosium complex," J. Lumin. **132**(4), 965–971 (2012).
25. S. J. Liang, J. P. Deng, and W. T. Yang, "Monomer reactivity ratio and thermal performance of alpha-methyl styrene and glycidyl methacrylate copolymers," Chin. J. Polym. Sci. **28**(3), 323–330 (2010).
26. A. Gill, C. Hong, D. Gromadzki, and M. Maric, "Reactive compatibilization of poly(styrene-ran-acrylonitrile)/poly(ethylene) blends through the acid-epoxy reaction," J. Appl. Polym. Sci. **133**(44), 457–463 (2016).
27. A. Q. Zhang, N. Q. Sun, L. P. Li, Y. M. Yang, X. J. Zhao, H. S. Jia, X. G. Liu, and B. S. Xu, "Tunable white light emission of Eu,Tb,Zn-containing copolymers by RAFT polymerization," J. Mater. Chem. C Mater. Opt. Electron. Devices **3**(38), 9933–9941 (2015).
28. Y. G. Lv, Y. H. Zhao, Z. W. Yang, C. J. Liu, H. Yan, G. Li, H. Liu, and J. Xie, "Luminescent property of a novel rare earth complex $Eu(TTA)_2NH_2$-$Phen_3$," Synth. Met. **159**(23–24), 2530–2533 (2009).
29. N. Q. Sun, X. J. Zhao, Y. M. Yang, L. P. Li, A. Q. Zhang, H. S. Jia, and X. G. Liu, "Synthesis and luminescent properties of terbium complex containing 4-benzoylbenzoic acid for application in NUV-based LED," J. Rare Earths **34**(2), 130–136 (2016).
30. M. Yamamoto, T. Nakanishi, Y. Kitagawa, K. Fushimi, and Y. Hasegawa, "Luminescent Eu(III) coordination polymer cross-linked with Zn(II) complexes," Mater. Lett. **167**, 183–187 (2016).
31. A. Fischer, T. Koprucki, K. Gartner, M. L. Tietze, J. Bruckner, B. Lussem, K. Leo, A. Glitzky, and R. Scholz, "Feel the Heat: Nonlinear Electrothermal Feedback in Organic LEDs," Adv. Funct. Mater. **24**(22), 3367–3374 (2014).
32. L. Yao, S. P. Wen, X. Duan, X. D. Hu, M. S. Che, W. F. Jing, H. L. Liu, and L. Liu, "Self-polymerization of $Eu(TTA)_3AA$ in rubber and their fluorescence effect," J. Rare Earths **31**(12), 1130–1136 (2013).
33. F. J. Zhang, Z. Xu, S. L. Zhao, L. Liu, W. W. Jiang, B. Sun, D. Liu, J. Z. Huang, and J. Pei, "Electroluminescence of $Tb(o\text{-}BBA)_3(phen)$ based on an organic-inorganic heterostructure," J. Lumin. **122-123**, 727–729 (2007).
34. A. Q. Zhang, Y. M. Yang, G. M. Zhai, H. S. Jia, and B. S. Xu, "Tuning the chromaticity of the emission color of the copolymers containing Eu(III), Tb(III), Be(II) ions based on colorimetric principle," Opt. Mater. **52**, 92–99 (2016).
35. M. Shang, C. Li, and J. Lin, "How to produce white light in a single-phase host?" Chem. Soc. Rev. **43**(5), 1372–1386 (2014).
36. F. Kang, Y. Zhang, and M. Peng, "Controlling the Energy Transfer via Multi Luminescent Centers to Achieve White Light/Tunable Emissions in a Single-Phased X_2-type Y_2SiO_5:Eu^{3+},Bi^{3+} Phosphor For Ultraviolet Converted LEDs," Inorg. Chem. **54**(4), 1462–1473 (2015).
37. M. L. Bhaumik and C. L. Telk, "Fluorescence quantum efficiency of rare-earthchelates," J. Opt. Soc. Am. B **54**(10), 1211–1214 (1964).
38. D. G. Deng, H. Yu, Y. Q. Li, Y. J. Hua, G. H. Jia, S. L. Zhao, H. P. Wang, L. H. Huang, Y. Y. Li, C. X. Li, and S. Q. Xu, "$Ca_4(PO_4)_2O$:Eu^{2+} red-emitting phosphor for solid-state lighting: structure, luminescent properties and white light emitting diode application," J. Mater. Chem. C Mater. Opt. Electron. Devices **1**(19), 3194–3199 (2013).

Optical Materials EXPRESS

39. C. H. Chiang, S.-J. Gong, T.-S. Zhan, K.-C. Cheng, and S.-Y. Chu, "Light-Emitting Diodes With High Color Rendering Index and Tunable Color Temperature Fabricated Using Separated Phosphor Layer Structure," IEEE Electron Device Lett. **37**(7), 898–901 (2016).
40. F. Zhang, X. Feng, Y. Zhang, L. Yan, Y. Yang, and X. Liu, "Photoluminescent carbon quantum dots as a directly film-forming phosphor towards white LEDs," Nanoscale **8**(16), 8618–8632 (2016).